Received: *December 4, 2001*, Accepted: *March 28, 2001*
Revised: *March 12, 2001*

A fresh look at diffractive J/ψ photoproduction at HERA, with predictions for THERA.

Leonid Frankfurt
Nuclear Physics Dept., School of Physics and Astronomy
Tel Aviv University, 69978 Tel Aviv, Israel
E-mail: frankfur@lev.tau.ac.il

Martin McDermott
Division of Theoretical Physics
Dept. Mathematical Sciences, Liverpool University
Liverpool L69 3BX, England
E-mail: martinmc@amtp.liv.ac.uk

Mark Strikman
Department of Physics, Penn State University
University Park, PA, 16802-6300, USA.
E-mail: strikman@phys.psu.edu

Abstract: We quantify perturbative and non-perturbative QCD effects in the exclusive J/ψ-photoproduction cross section, and in the shrinkage of the differential cross section with respect to momentum transfer, t. We predict that in the high energy THERA region there will always be a significant contribution to this process that rises quickly with energy. This implies that the taming of the rise of the cross section with energy, due to both the expansion of spatially-small fluctuations in the photon and to higher twist effects, is rather gradual.

Keywords: QCD, Heavy Quarks Physics, LEP HERA and SLC Physics.

JHEP03(2001)045

Contents

1. Introduction

One of the major challenges facing particle physics is to understand the interplay of perturbative and non-perturbative QCD effects in the high-energy production of heavy quark bound states and in the interaction of such states with hadrons. Understanding the details of this interplay is interesting in its own right because it reveals the practical boundaries of applicability of perturbation theory. It is also necessary to achieve an unambiguous interpretation of many related phenomena, including the suppression of the yield of J/ψ mesons produced in nucleus-nucleus collisions. The investigation of hard exclusive processes, such as the exclusive photoproduction of the J/ψ meson in photon-proton collisions considered here, gives a unique opportunity to quantify this physics.

For several years, high energy, hard exclusive and semi-inclusive processes, which include photo- and electroproduction of heavy vector mesons and deep inelastic production of light vector mesons and real photons (DVCS), have been modelled reasonably successfully using the exchange of two gluons in a colour singlet configuration [1]–[8].

For vector meson production initiated by longitudinally polarised photons [3, 9] and for DVCS [10] such calculations have now been placed on a firmer theoretical footing by the proof of QCD factorization theorems which show that perturbative two gluon exchange is the dominant process in the asymptotic limit ($Q^2 \to \infty$).

To make a process "hard" it is necessary to provide a large momentum scale (either a heavy quark mass or Q^2, or both) which squeezes the hadronic fluctuation of the photon so that small perturbative $q\bar{q}$ configurations are responsible for the dominant contribution. For the diffractive photoproduction of J/ψ this hard scale is thought to be provided by the charm mass. However, since the charm quark is rather light ($m_c \approx 1.5\,\mathrm{GeV}$), and transverse polarisations of the quasi-real photon dominate, there are likely to be significant contributions from non-perturbative regions in which the hadronic fluctuation of the photon has a large transverse size (these become progressively less important as the photon virtuality increases). This interplay between soft and hard contributions has been seen in a phenomenological way by the success of the two-Pomeron fit of Donnachie and Landshoff [11] in which the soft Pomeron term, associated with non-perturbative effects, appears make a significant contribution to J/ψ photoproduction at HERA energies.

At very high energies, or small x_{Bj}, the time taken for a given fluctuation in the photon to interact with the proton target is considerably smaller than its formation time and the time required to produce the hadronic final state. This implies universality for the interaction cross section over a wide range of inclusive and exclusive processes. In [12] we introduced a model for this universal cross section, $\hat{\sigma}$, for all transverse size fluctuations.[1] We produced a satisfactory description of the inclusive cross section data, indicating that our model is reasonable. In this paper, having made some suitable minor adjustments, we apply the model to J/ψ photoproduction. Our aim is twofold, to provide a good description of this process (and hence to elucidate the role of non-perturbative physics in J/ψ photoproduction) and to further constrain the model in order to be able to make better predictions for other exclusive processes in the future, using the same framework.

Our model for the interaction cross-section is based on the well-known leading-log perturbative QCD result for the interaction of a small transverse-size $q\bar{q}$ dipole which proceeds via two-gluon exchange [13]:

$$\hat{\sigma}_{pQCD}(b^2, x) = \frac{\pi^2}{3}\, b^2\, \alpha_s(\bar{Q}^2)\, xg(x', \bar{Q}^2)\,, \tag{1.1}$$

where scales x' and $\bar{Q}^2$, which depend on transverse size b, are described in subsection 3.1. This form is applicable for transverse sizes $b < b_{Q0} \approx 0.4\,\mathrm{fm}$. For

[1] Modelling is currently unavoidable in QCD due to the necessity to take non-perturbative confinement effects into account. We defer a more detailed modelling of the strong interaction in the region of small α_s, which seems to be required for the very small-x regime in which Structure Functions may achieve the unitarity limit, for future studies.

larger transverse sizes we introduced an ansatz based on the known behaviour of soft hadronic interactions (we matched on to the measured πp cross section at $b = b_\pi = 0.65\,\text{fm}$) and introduced a suitable interpolation for $b_{Q0} < b < b_\pi$ and an extrapolation for $b > b_\pi$. In this paper we slightly simplify the model for $\hat{\sigma}$ by connecting the points b_{Q0} and b_π with a straight line (instead of extrapolating a fit to the known b-shape just below b_{Q0} as in [12]). At very high energies, we tame the steep increase due to the rapid rise of the small-x gluon density by imposing a unitarity restriction, $\sigma(b_1, W^2) = \sigma(b_\pi, W^2)/2$, and connect the point $b_1 < b_{Q0}$ to b_π using a straight line (see figures 7, 13 and subsection 3.4 for more details).

We use this model, based on eq. (1.1) with CTEQ4L [14] gluon input density, evolved using skewed evolution, to investigate the interplay of perturbative and non-perturbative effects in J/ψ photoproduction.[2] At the higher photon-proton energies of the HERA range ($W \approx 250\,\text{GeV}$) this involves probing the gluon distribution at very small $x \approx 10^{-4}$, i.e. outside of the range in which it has been tested directly. In this region, it is mainly constrained indirectly by its effect on the observed scaling violations of the inclusive structure function F_2, predicted by DGLAP [15] evolution. It should be remembered that the predictions we make would change if the input gluon density is changed. Indeed, in our final plot for the cross section we also show the results using the latest MRST leading order partons [16].[3] Taken together, the predictions using both CTEQ4L and MRST produce a spread which spans the currently available data. Other models for the interaction cross section, $\hat{\sigma}$, may be found in the literature (see e.g. [18, 19] and references therein).

The amplitude for exclusive processes involves a convolution of $\hat{\sigma}$ with light-cone wavefunctions for the initial-state photon (known from QED [20] in the $q\bar{q}$ case) and for the final-state diffractively-produced object. For the light-cone wavefunction of the J/ψ we use a hybrid wavefunction introduced in [4]. This is derived by solving the Schrödinger equation using the Buchmueller-Tye potential model [21] (constituent quark mass $m_c = 1.48\,\text{GeV}$), boosting the resulting Schrödinger wavefunction to a fast moving frame. The wave function at small $b < 0.3$ fm is fixed by imposing QCD behaviour ($\phi_V(z, b = 0) \propto z(1-z)$) and normalized using the known leptonic decay rate of J/ψ. In this way we account for the QCD radiative corrections to the $q\bar{q}$ component of the charmonium wavefunction for small transverse sizes $b < 0.3\,\text{fm}$. This effectively takes into account the strong modification of non-relativistic charmonium-model predictions for the leptonic width due to QCD radiative corrections (for a recent review see [22]). The exclusive formation of the heavy bound state, the details of which are embodied in the light-cone wavefunction,

[2]The value of $\hat{\sigma}_{pQCD}(b^2, x)$ should not change significantly within the next-to-leading order approximation, as compared to the leading order, because it is determined from fitting the same value of F_2. However, both the relative size of $\hat{\sigma}_{pQCD}(b^2, x)$ and $xg(x, Q^2)$ and the numerical value of $xg(x, Q^2)$ itself may change rather significantly.

[3]This leading order input distribution is more recent than, but similar to, that found in [17].

JHEP03(2001)045

suppresses the contribution of higher order Fock states (such as $|c\bar{c}g\rangle$) in the virtual photon, making this a particularly good process in which to test the universality of the dipole picture.

For small enough x, the rapid rise of $\hat{\sigma}$ due to the small-x rise of the gluon density should be tamed to avoid violating the unitarity restriction for the interaction of spatially-small partonic fluctuations of the photon. Two types of effects act to tame the increase of high energy processes. As the energy increases, spatially-small partonic fluctuations in the photon typically expand rapidly in transverse size due to the increased phase-space for radiation. This expansion in size, known as Gribov diffusion, is a consequence of the randomness of radiation. For large size configurations perturbative QCD is inapplicable so the amplitudes no longer have this fast increase with energy. We account for Gribov diffusion to some extent by implementing a behaviour typical of soft hadronic cross sections (i.e. with only mild increase with energy) at large transverse sizes. Even if $\hat{\sigma}$ is completely independent of b^2 at sufficiently small-x the Structure Function of a hadronic target should retain a residual $\ln(1/x)$ increase with energy as a result of the infinite normalization of the wavefunction of a virtual photon (the infinite renormalization of electric charge is due to hadronic vacuum polarisation). Another effect is taming, or shadowing, of the rapid rise with energy due to higher twist effects. So, for small enough x, unitarity corrections were introduced in [12] to tame the rapid rise of $\hat{\sigma}$ due to the small-x rise of the gluon distribution. These affect larger transverse sizes in the perturbative domain first. If perturbative QCD effects are tamed by the unitarity of S-matrix only, this mechanism would lead to an increase of the typical impact parameters, ρ, involved in the scattering of $q\bar{q}$ dipole from a nucleon as $\rho^2 \propto \ln^2 1/x$ and leads to a related increase of Structure Functions as $F_2 \propto (\ln 1/x)^3$ (and $\alpha' \propto \ln^2 1/x$).

In this paper, we illustrate that the photoproduction of the relatively light J/ψ can act as a precursor for this taming since it is sensitive to relatively large transverse sizes, not just to the wavefunction at the origin [4, 5]. Thus, we consider the behaviour of the energy dependence of the cross section of J/ψ-photoproduction (especially that of the slope of the momentum transfer, t, which is parameterised by $\alpha'_{I\!P}$) to be crucial in establishing the existence of a new regime in which the standard DGLAP approximation is violated. Remember that the slowing down of the increase of the Structure Function alone does not necessarily imply violation of DGLAP, because it may be due to Gribov diffusion, which is a leading twist phenomenon. We note in passing that an important role of large transverse distance effects (soft QCD) reveals itself in the energy dependence of the slope for the photoproduction of J/ψ mesons which, within our model, should be intermediate between the soft regime, $\alpha'_{I\!P}(\text{soft}) \sim 0.25 \text{ GeV}^{-2}$, and the perturbative regime, $\alpha'_{I\!P} \ll \alpha'_{I\!P}(\text{soft})$ (see subsection 3.3 and section 6).

We predict a reduction in the steepness of the energy dependence of amplitudes of hard exclusive processes which will begin to take effect at the higher HERA energies and in the THERA region ($250 \leq W \geq 1000\,\mathrm{GeV}$). The precise details are of course specific features of our model,which incorporates a simple taming ansatz in the small x region. More generally, taming corrections are eventually expected to reduce the rise with energy of all hard small-x cross sections at given impact parameter.[4]

This paper extends the work of [5, 6] in two original directions. Firstly, it explicitly includes the non-perturbative component coming from large transverse sizes and provides a reasonable unified description of the process from the low energies measured at fixed target experiments [23] as well as the HERA data [24]–[26]. Within the framework of our analysis the relative contribution of non-perturbative effects may be quantized, albeit in an inevitably model-dependent way. Secondly, we make predictions for energies beyond the HERA range $W \gtrsim 300$ GeV that may eventually be tested at a higher energy ep collider such as the proposed Tesla-HERA, or THERA, project (see e.g. [27]). The logic of [12] dictates that taming corrections are required in this high energy region and we qualify and quantify the expected effect of these corrections on J/ψ photoproduction.

The paper is organized as follows. Section 2 contains the basic formula for the cross section. Section 3 investigates various issues surrounding the implementation of this formula including setting scales in the gluon distribution, running quark mass effects, $t-$dependence, skewedness and the calculation of the real part of the amplitude. In section 4 we illustrate the effect of changing the rescaling parameter λ, in the model for the dipole cross section. Section 4 also contains our predictions for the THERA energy range. Following a discussion and evaluation of $\alpha'_{I\!P}$ in section 5, we include a general discussion in section 6 and conclude in section 7.

2. Basic formulae in the photoproduction limit

From [5, eq. (50)] in the limit $Q^2 \to 0$, neglecting the real part of the amplitude, the differential cross section for the photoproduction of J/ψ reads:

$$\frac{d\sigma}{dt}\,|_{t=0} = \frac{12\pi^3 \Gamma_V M_V^3}{\alpha_{e.m}(4m_c^2)^4}\,\left[\frac{\pi^2}{3}\alpha_s(Q^2_{\text{eff}})xg(x,Q^2_{\text{eff}})\right]^2\,\left(\frac{3}{\pi^2}\right)^2 C(Q^2=0)\,, \tag{2.1}$$

where M_V, Γ_V are the mass and leptonic decay width of the vector meson and $m_c = 1.5$ GeV is the charm quark mass. Using the notation of [5] (in particular eqs. (25,26,51)) we have for the overall dimensionless suppression factor

$$C(Q^2=0) = \left(\frac{\eta_V m_c^4}{3}\right)^2 T(0)R(0)\,, \tag{2.2}$$

[4]However, it is unclear whether the unitarity of S-matrix for the interaction of small size fluctuations should tame the increase with energy of Structure Functions, because of the related increase of the important impact parameters with energy. This question will be investigated in a separate publication.

$$T(0)R(0) = \frac{1}{M_V^4} \frac{\left[\int (dz/z(1-z)) \ \int db \ b^3 \ m_{c,r}^2 \ \phi_V \ \phi_\gamma^T\right]^2}{\left[\int (dz/z(1-z)) \ \phi_V(z, b=0)\right]^2}, \tag{2.3}$$

$$\left(\frac{\eta_V}{3}\right)^2 = \left(\frac{\int (dz/z(1-z)) \ \phi_V(z, b=0)}{6 \int dz \ \phi_V(z, b=0)}\right)^2, \tag{2.4}$$

where $m_{c,r}(b)$ is the running charm quark mass and ϕ_γ^T, ϕ_V are the light-cone wavefunctions for the transversely-polarised photon and vector meson, respectively. The latter depend on transverse size b, and on z, the momentum fraction of the photon energy carried by the quark. In eq. (2.1) the gluon density and α_s have been extracted at the average point, $\langle b \rangle$, of the integration over b in the amplitude, using the relationship $Q^2_{\rm eff} = \lambda/\langle b^2 \rangle$, with $\lambda \approx 10$. In [6] we attempted to go further than this average approximation by sampling these functions at the $\bar{Q}^2 = \lambda/b^2$, underneath the integral in transverse size b. The factor $m_{c,r}^4$ implicitly depends on b, so rightfully also belongs underneath the integral in b, sampled at an appropriate scale.

Reinstating $\hat{\sigma}$ underneath the integral according to this procedure leads to a modified version of eq. (2.1):

$$\begin{aligned}
\frac{d\sigma}{dt}\Big|_{t=0} &= \frac{12\pi^3 \Gamma_V}{\alpha_{e.m} 6^2 4^4 M_V} \frac{9}{\pi^4} \frac{\left[\int (dz/z(1-z)) \int b \ db \ m_{c,r}^2 \ \phi_\gamma^T \ \hat{\sigma} \ \phi_V\right]^2}{\left[\int dz \phi_V(z, b=0)\right]^2}, \\
&= \frac{1}{16\pi} \frac{3}{16} \left[\frac{\Gamma_V}{\alpha_{e.m} M_V [\int dz \phi_V]^2}\right] |\Im m \ \mathcal{A}|^2, \\
&= \frac{1}{16\pi} \frac{3}{16} \left[\frac{32\pi \alpha_{e.m} e_c^2}{M_V^2}\right] |\Im m \ \mathcal{A}|^2 \\
&= \frac{N^2}{16\pi} |\Im m \ \mathcal{A}|^2,
\end{aligned} \tag{2.5}$$

where the penultimate line makes use of eq. (40) of [5]. The imaginary part of the amplitude, $\Im m \ \mathcal{A}$, and its normalization, N, are given by

$$N^2 = \frac{6\alpha_{e.m} \pi e_c^2 m_c^4}{M_V^2}, \tag{2.6}$$

$$\Im m \ \mathcal{A} = \int b \ db \ I_z(b) \ \hat{\sigma}, \tag{2.7}$$

$$I_z(b) = \int_0^1 \frac{dz}{z(1-z)} \ \left(\frac{m_{c,r}(b)}{m_c}\right)^2 \ \phi_\gamma^T \ \phi_V, \tag{2.8}$$

where the light-cone wavefunction for the photon, $\phi_\gamma^T = K_0(b \ m_{c,r})$, is purely transverse for photoproduction. In this equation we have chosen to separate out a piece of the b-integral, $I_z(b)$, which only depends on the light-cone wavefunctions of the vector meson and photon and is independent of energy.

For small dipole sizes $b < 0.3$ fm QCD behaviour is imposed [5] on $\phi_{J/\psi}$, so it is appropriate to run the charm quark mass underneath the b-integral too, in both the

JHEP03(2001)045

overall $m_{c,r}^2$ factor and in the argument of the Bessel function, using the appropriate renormalization group equation for masses (see subsection 3.2).

Finally, assuming the usual exponential fall-off in t we have

$$\sigma(\gamma P \to J/\psi\ P) = \frac{N^2(1+\beta^2)|\Im m\ \mathcal{A}|^2}{16\pi B}, \tag{2.9}$$

where the real part of the amplitude has been reinstated via $\beta = \Re e\ \mathcal{A}/\Im m\ \mathcal{A}$ (see subsection 3.5). The H1 collaboration recently reported [24] a value of $B = 4.73 \pm 0.25\ {}^{+0.30}_{-0.39}$ GeV^{-2}. Recently ZEUS reported [25] an improved measurement of B in J/ψ photoproduction and found it to depend on energy. We will incorporate this shrinkage using a simple form (see subsection 3.3).

3. Improvements to the basic formula: uncertainties in the cross section

In this section we expand and explain various features and uncertainties in the basic formulae of section 2. Many crucial issues involve the b-integral in eq. (2.7). Firstly we explain the choice of scales, x', $\bar{Q}^2$ used in the dipole cross section and make a first comparison to the available data, using very basic assumptions. Then we consider the changes induced by considering a more careful treatment of running mass effects, shrinkage, non-zero real part and skewedness. The latter requires that we replace the ordinary gluon with the skewed gluon in eqs. (1.1), (2.7). We follow the usual choice of conventional input distributions evolved using skewed evolution.

Lastly, in the next section, we decrease the parameter λ which relates transverse sizes to four-momentum scales, via $Q^2 = \lambda/b^2$, from 10 to 4. This has the effect of increasing the non-perturbative contribution to the cross section and leads to a much better description of the current data. We also give predictions for THERA for both values of λ.

3.1 Scale setting in the gluon density

In [12] we examined inclusive structure functions, F_L and F_2, using our model for $\hat{\sigma}$. We employed the following prescription for the b-dependence of the scales x' and $\bar{Q}^2$:

$$x' = x'_{\min}\left(1 + 0.75\frac{\langle b\rangle^2}{b^2}\right), \tag{3.1}$$

$$\bar{Q}^2 = \frac{\lambda}{b^2}, \tag{3.2}$$

with,

$$x'_{\min} = x_{Bj}\left(1 + \frac{4m_q^2}{Q^2}\right),$$

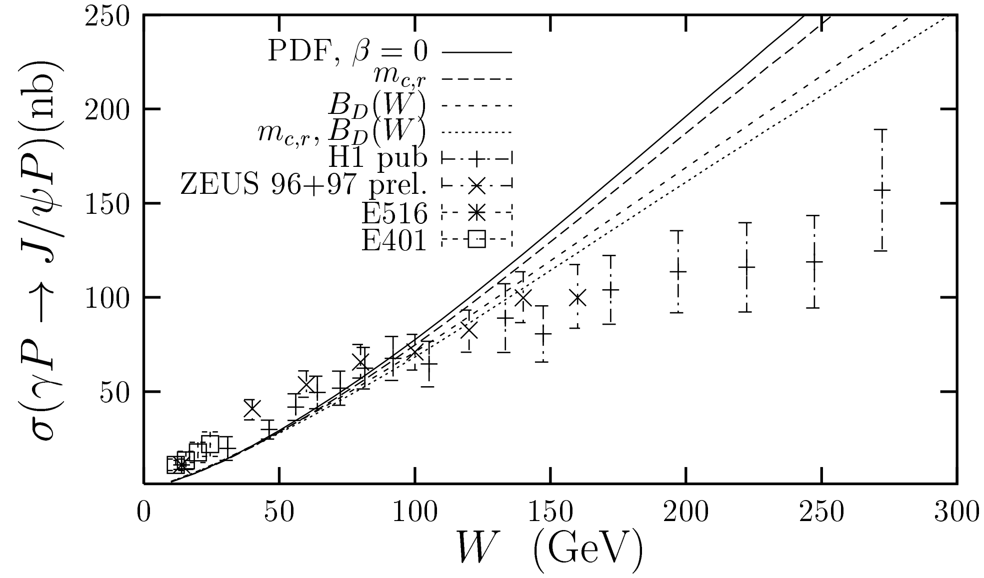

Figure 1: A comparison of the J/ψ photoproduction cross section, using conve ntional CTEQ4L parton distribution function (PDF) for the gluon and $\beta = 0$, with data [23, 24, 25, 26]. The solid curve has fixed mass and slope $B = 4.0$ GeV^{-2}, the long and short dashed curves include runnin g charm quark mass and W-dependent slope, respectively. The dotted curve includes both effects.

$$\langle b \rangle^2 = \frac{\lambda}{Q^2 + 4m_q^2} . \tag{3.3}$$

By examining the standard perturbative QCD formula for F_L for light quarks we found $\langle x \rangle \approx 1.75\, x$ (we designed the ansatz to reproduce this for large Q^2 when $b = \langle b \rangle$). We also found that a value of $\lambda = 10$ reproduced the perturbative QCD results fairly well. However the results turned out to be rather insensitive to the precise value of λ. In this paper we explicitly examine the sensitivity of J/ψ photoproduction on λ and find that it is much more sensitive to it than F_L and F_2 (see section 4). This is interesting because the value of λ determines the dividing line between perturbative and non-perturbative physics.

In the photoproduction limit, $Q^2 \to 0$, for charm eqs. (3.1), (3.3) lead to

$$x' \to \frac{4m_c^2}{W^2}\left(1 + 0.75\frac{\lambda}{b^2 4m_c^2}\right) , \tag{3.4}$$

for the $b-$dependent momentum fraction of the incoming gluon. This will be used for the sampling of $\hat{\sigma}$ underneath the b-integral in eq. (2.7).

The solid line in figure 1 shows the resulting J/ψ photoproduction cross section using eq. (2.9), with CTEQ4L gluon density, $\beta = 0$, a fixed slope parameter of

$B = 4.0\,\mathrm{GeV}^{-2}$ and fixed quark mass of 1.5 GeV. The available data [23]–[26] is also shown. This curve undershoots the data at low energies and overshoots at high energies, so it appears to rise too steeply with energy to provide a good description of all available data. We now consider several features which improve the shape of the energy dependence.

3.2 Running quark mass

In [5] hard QCD corrections were introduced in the vector meson wavefunction: for $b < b_0$ ($b_0 = 0.3$ fm was chosen for J/ψ) QCD-behaviour was imposed ($\phi_V \propto z(1-z)$) and normalized to the measured leptonic decay width. For consistency it was then necessary to replace the constituent quark mass with the running quark mass for small b. This was implemented in the following way: (cf. [5, eq. (38)])

$$m^2 \to m_{c,r}^2(Q_{\text{eff}}^2) = m_c^2 \left(1 - \frac{8\alpha_s(Q_{\text{eff}}^2)}{3\pi}\right).$$

In this paper, we demand that the mass satisfies the renormalization group formula for quark masses (see e.g. [28]):

$$m_{c,r}(\bar{Q}^2) = m_c \left(\frac{\alpha_s(\bar{Q}^2)}{\alpha_s(\bar{Q}_f^2)}\right)^{12/33-2n_f}, \tag{3.5}$$

where $Q_f \approx 2.0\,\mathrm{GeV}$ corresponds to the matching scale, $b_0 = 0.3\,\mathrm{fm}$, at which hard corrections are applied. We set the number of flavours $n_f = 4$ both in the exponent and in the one-loop beta-function of α_s (choosing $n_f = 3$ instead would make very little difference). This effect suppresses the small b region relative to the case in which the mass is taken as fixed, imposing the desired QCD behaviour $m_c \to 0$ for $\bar{Q}^2 \to \infty$. Figure 2 shows $m_{c,r}^2(b)/m_c^2$ versus b. We use $m_c = 1.5$ GeV, which is approximately the constituent quark mass of Buchmueller-Tye potential model [21], which we use to construct ϕ_V. Figure 3 illustrates the size of the effect at the amplitude level. Running the quark mass influences both the argument of the K_0 Bessel function and the overall multiplicative factor in eq. (2.8). It turns out that there is only significant suppression for $b < 0.2\,\mathrm{fm}$ (rather than $b < b_0 = 0.3$ fm). A comparison of the solid and long-dashed lines of figure 1 illustrates the rather small decrease that this change induces in the cross section as a result of the reduced contribution from small b.

3.3 Energy dependent slope

We shall evaluate this effect in detail in the section 5. Here we give a brief outline of the significance of the energy dependence of the slope of the t-dependence. The recent presentation of ZEUS data, from the 1996-97 running period, at DIS2000 [25, 26] indicated evidence for shrinkage. Following a fit to $d\sigma/dt$ of the form $\exp(Bt)$ in each of the seven bins in W, a value of $\alpha'_{I\!P} = 0.098 \pm 0.035 \pm 0.05\,\mathrm{GeV}^{-2}$ is obtained

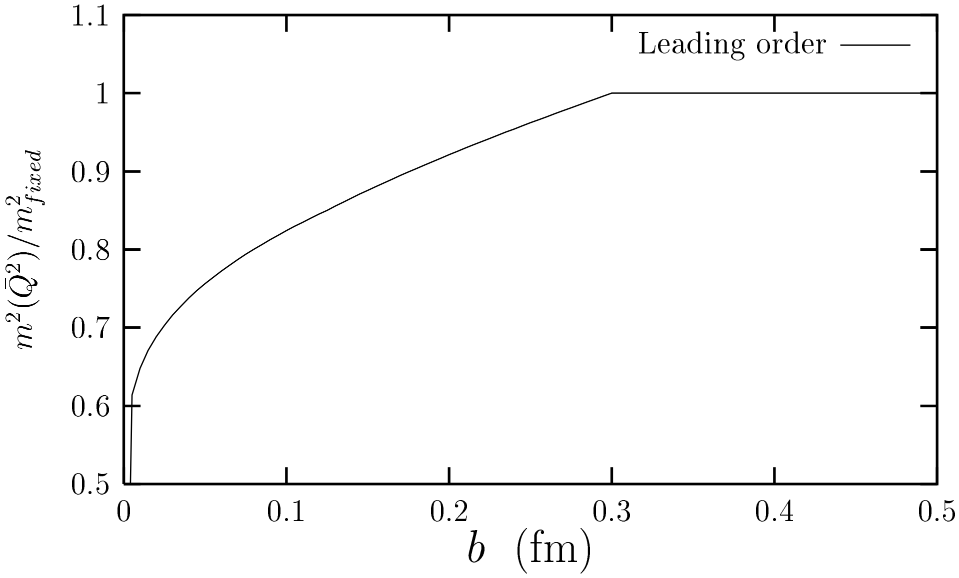

Figure 2: The ratio of running charm quark mass squared to fixed mass squared as a function of transverse size using eq. (3.5) and incorporating four light flavours, $n_f = 4$.

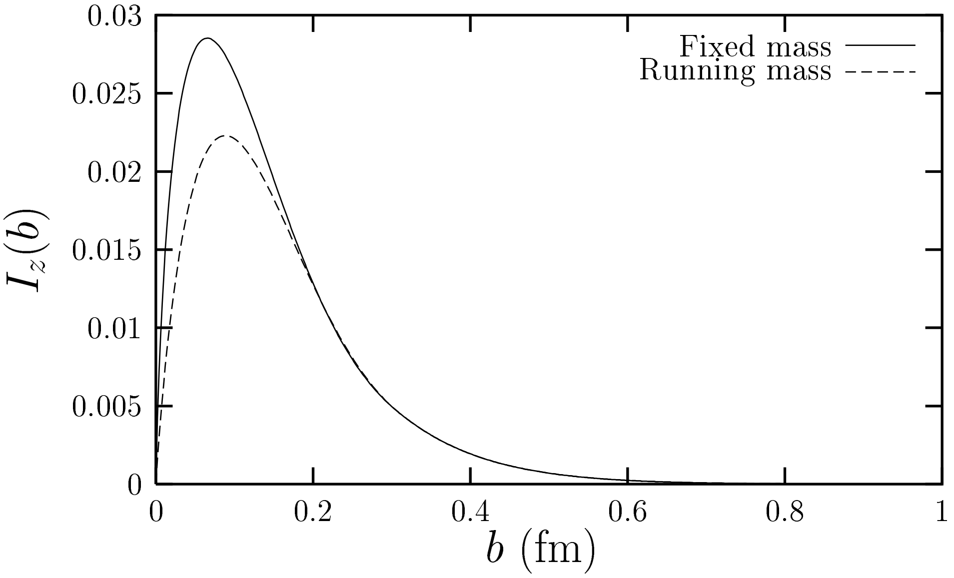

Figure 3: The integrand multiplying $\hat{\sigma}$ for fixed and running charm quark mass. The running mass effect is implemented for $b < 0.3\,\mathrm{fm}$ and causes a suppression of the small b region.

from examining the energy dependence of B. In order to take this into account we use the following form for the energy-dependent slope parameter

$$B(W) = B(W_0) + 2\ \alpha'_{I\!P}\ \ln(W/W_0)^2\,, \tag{3.6}$$

with $B(W_0) = 4.0\ \mathrm{GeV}^{-2}$ at an input scale of $W_0 = 40\,\mathrm{GeV}$ and following ZEUS we take $\alpha'_{I\!P} = 0.1\,\mathrm{GeV}^{-2}$. This clearly implies a reduction in the overall normalization of the cross section at large W, relative to the case in which a constant B is employed (for $W = 200$ GeV the reduction is about 14 %).

A comparison of the short-dashed and solid lines of figure 1 show the significant effect of including the W-dependent slope according to eq. (3.6). The dotted curve shows the combined effect of running quark mass and $B(W)$ on the solid curve (cf. also eq. (3.5)). Both effects reduce the steepness of the energy dependence bringing the theory curves closer to the data.

3.4 Skewedness

Strictly speaking for exclusive processes we need to replace the ordinary gluon in eq. (1.1) with the skewed gluon $G(x_1, \delta, \bar{Q}^2)$ (see [29], and references therein, for a review of skewed parton distributions). For J/ψ this should have a rather small effect, for Υ, with its much larger mass, it is certainly a large effect [6]. It is not obvious precisely how to sample the skewed gluon. Assuming collinearity of the incoming and returning gluons (carrying momentum fractions x_1 and $-x_2$ of the proton, respectively) we have $(x_1 P + q)^2 = M^2_{c\bar{c}}$, $((x_1 - x_2)\ P + q)^2 = M^2_V$. In the photoproduction limit for the skewedness parameter, δ, this gives

$$\delta = x_1 - x_2 = \frac{M_V^2}{W^2}\,, \tag{3.7}$$

$$x_1 = \frac{M^2_{c\bar{c}}}{W^2} = \delta \frac{(m_c^2 + k_t^2)/\ z(1-z)}{M_V^2}\,. \tag{3.8}$$

At first sight it appears there may be a danger of entering the ERBL [30] region ($x_1 < \delta, x_2 < 0$) in certain points in the phase space (in particular for symmetric, $z \approx 1/2$, configurations with small k_t^2). However, our ansatz protects us from this, in the case of J/ψ, since we only use eq. (1.1) for $b < b_{Q0}$, which corresponds roughly to $k_t^2 > Q_0^2$. Even for an input scale of 1.0 GeV^2 this implies $M^2_{c\bar{c}} > 4(m_c^2 + Q_0^2) > 13.0\,\mathrm{GeV}^2$. This is much bigger than the square of the J/ψ mass: $M^2_\psi(1S) = 9.59\,\mathrm{GeV}^2$. The 2S-state, ψ', with a mass of $M^2_{\psi'}(2S) = 13.59\,\mathrm{GeV}^2$ is a more marginal case, which merits further investigation.

For J/ψ photoproduction we will use

$$x' = x_1 = \delta\left(1 + 0.75 \frac{\lambda}{b^2\ 4m_c^2}\right) \tag{3.9}$$

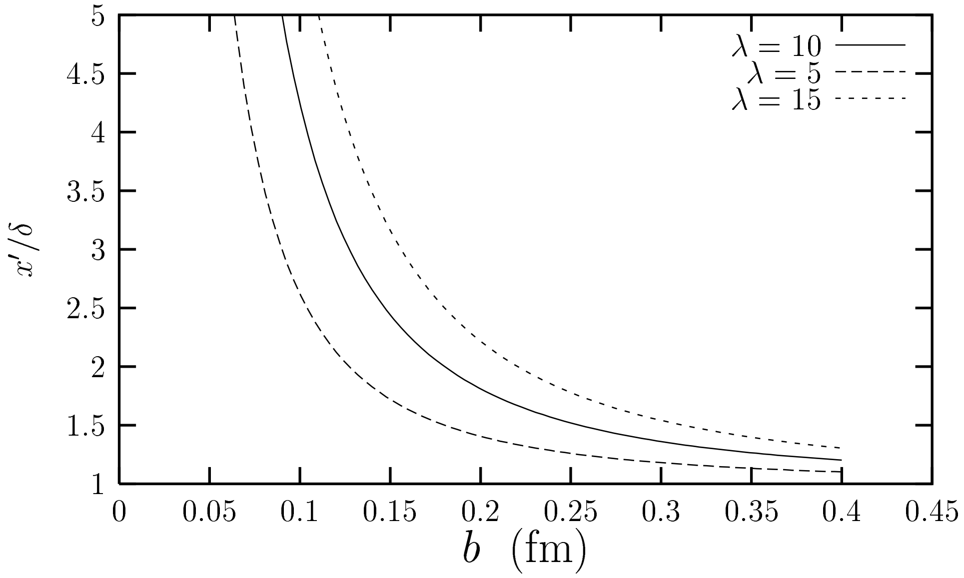

Figure 4: The effective momentum fraction at which the gluon is sampled, divided by δ, for several values of the scaling parameter λ.

(cf. eq. (3.1) with $x'_{\rm min} = \delta = M_V^2/W^2$). This choice obviously guarantees that $x' > \delta$ for all b, so restricts us just to the DGLAP region (with this assumption we can never enter the ERBL region). With $\lambda = 10, m_c = 1.5\,\text{GeV}$, $\langle b\rangle^2 = 10 * (hc)^2/4m_c^2 \approx (0.21$ fm$)^2$ and this reduces to

$$x'(b) = \delta\left(1 + \frac{0.032}{(b\ (\text{fm}))^2}\right). \tag{3.10}$$

In our computer codes, the divergence at $b \to 0$, in the numerically unimportant very small b-region, is regulated by hand by adding a very small number to b^2 in the denominator. The skewed gluon density, $G(x', \delta, \bar{Q}^2)$, is sampled at four-momentum scale $\bar{Q}^2 = \lambda/b^2 \approx 0.39/(b\ (\text{fm}))^2\ \text{GeV}^2$, hence some regulation of this scale is also implemented at very small b^2 (in practice we don't let the scale get larger than $\bar{Q}^2 = 100\,\text{GeV}^2$). Figures 4, 5 illustrate the b-dependence of x'/δ and $\bar{Q}^2$ for different values of parameter λ.

In order to implement skewedness we use the evolution package developed by Freund and Guzey [31], which is based on the CTEQ code [32]. The skewed parton distributions (SPDs) are implemented in a systematic way underneath the integral in b. For a particular value of W, δ is fixed. For this fixed δ, the skewed gluon is sampled on a grid, $G(x', \delta, Q^{2\prime})$ and the values saved to an array. The integration over b is performed numerically folding in the W^2-independent piece from the wavefunctions with $\hat{\sigma}$ calculated by interpolating the skewed gluon array appropriately using a

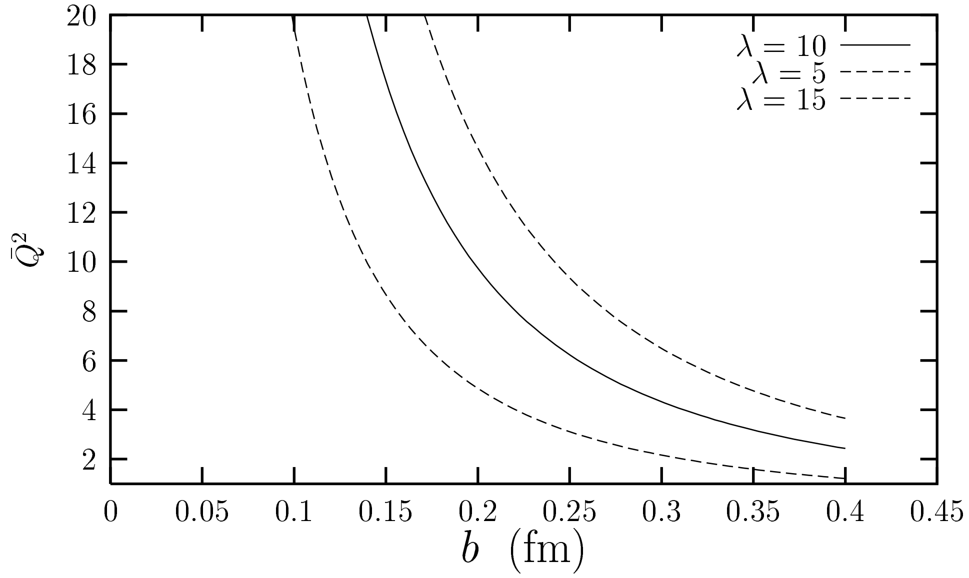

Figure 5: The effective four-momentum scale at which the gluon is sampled for several values of the scaling parameter λ.

splines-based interpolation routine. Figure 6 shows the skewed gluon versus the conventional one at a scale typical for J/ψ photoproduction for x' close to, but larger than, $\delta = 9.6 \times 10^{-4}$ (the value which corresponds to $W = 100$ GeV). Also shown is the SPD with very small $\delta = 10^{-7}$ which coincides with the conventional PDF, illustrating the limit $G \to xg$ as $\delta \to 0$.

Following closely the prescription for $\hat{\sigma}$ given in [12] we impose the following behaviour at $b = b_\pi$:

$$\sigma(b_\pi, W^2) = \sigma(b_\pi, W_0) \left(\frac{W^2}{W_0^2}\right)^\epsilon \tag{3.11}$$

with $\sigma(b_\pi, W_0) = 24$ mb, $\epsilon = 0.08$ and $W_0 = 31$ GeV. The latter value is chosen to coincide with the choice $x_0 = 0.01$ made in [12]. A simple linear ansatz is used for the skewed $\hat{\sigma}$ in the region $b_{crit} < b < b_\pi$ (we connect b_{crit} and b_π with a straight line, b_{crit} is the point in b at which $\sigma(b, W^2) = \sigma(b_\pi, W^2)/2$). For small W^2 taming isn't required in the perturbative region, $b < b_{Q0}$, so the straight line starts at b_{Q0}. The dashed lines of figure 7 show the effect of including skewedness in the dipole cross section relative to using the standard PDF (solid lines) at $W = 100, 300\,$GeV.

Close to the boundary at $b = b_{Q0} = 0.39$ fm, $x' \approx \delta$ and $\bar{Q}^2 \approx Q_0^2$. If one assumes the standard input at the boundary for skewed evolution as we do, the difference between the use of skewed and standard distributions is minimal close to b_{Q0}. For very small b, although there is a large evolution scale, $\bar{Q}^2 \gg Q_0^2$, the

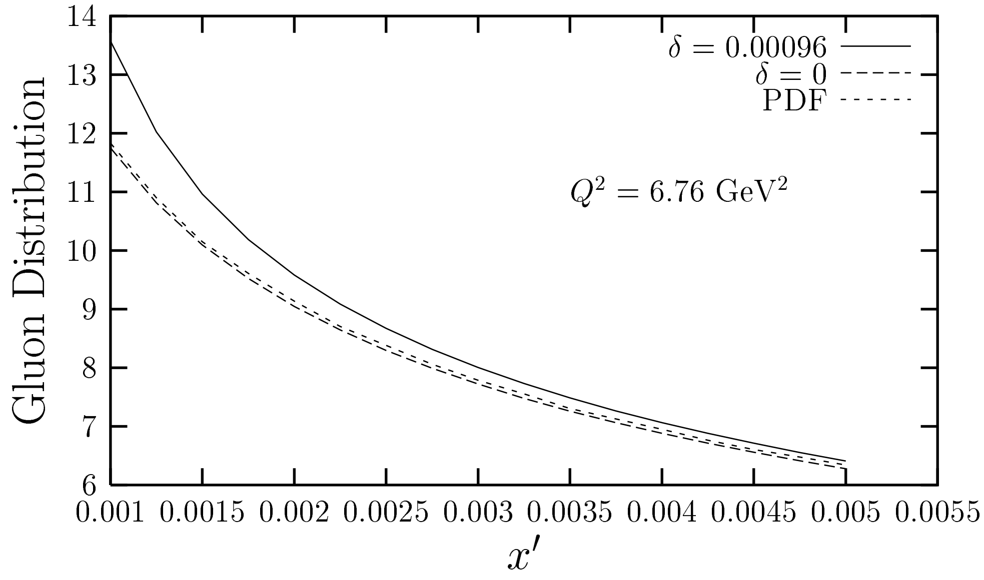

Figure 6: Skewed and conventional (PDF) gluon distributions at a scale typical of J/ψ photoproduction, $Q^2 = 6.76\,\mathrm{GeV}^2$. The value of $\delta = 0.00096$ corresponds to $W = 100\,\mathrm{GeV}$. This figure explicitly illustrates that the skewed distribution reduces to the standard one in the limit of zero skewedness.

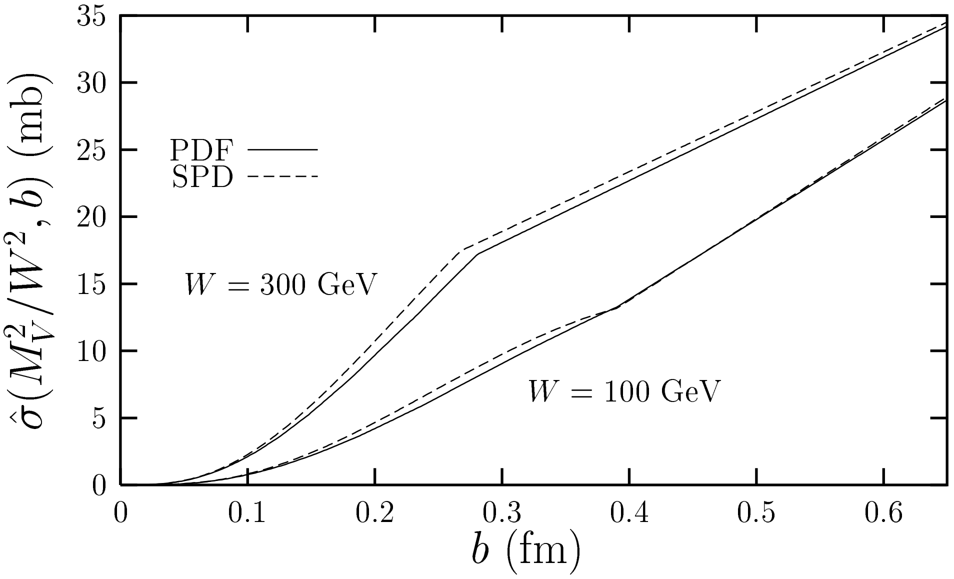

Figure 7: The dipole cross section $\hat{\sigma}$ including skewedness (dashed curves) and without (solid curves) for two photon-proton energies.

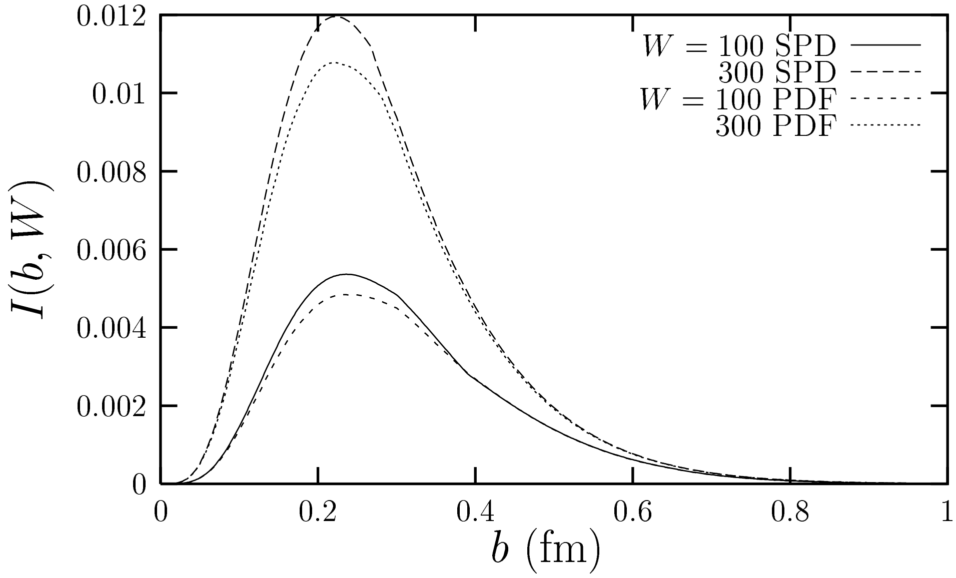

Figure 8: A comparison of the b-integrand of eq. (2.7) with (SPD) and without (PDF) skewedness at two different photon-proton energies.

gluon is sampled at $x' \gg \delta$, so the overall effect of skewedness is expected to be fairly small everywhere. This is illustrated explicitly in figure 8 which shows the integrand of eq. (2.7) using skewed and standard gluons at two different energies ($W = 100, 300\,\mathrm{GeV}$). The maximum effect, of about 10%, is seen close to the peak.

For the skewed case it is interesting to show how the b-distribution changes with energy, since this reflects the interplay of short and long distance contributions at different energies. One observes in figure 9 that the peak shifts to the left as the energy increases and becomes more narrow, indicating an increase in the relative importance of short distance effects in this region. Examining such plots at very high energies reveals how the unitarity corrections begin to set in. One can start to see this in the shape of the curves at $W = 300, 500$ GeV, where the taming restriction begins to remove part of the distribution to the right of the peak. Although the taming corrections start to bite around 300 GeV they take a long time to tame the majority of the (fairly broad) peak in b. In practice this implies that we expect the energy dependence to be tamed very gradually to the soft Pomeron one.

Finally, in figure 10 we show the effect of including skewedness at the cross section level. The solid line corresponds to standard gluon PDF in $\hat{\sigma}$ (with running mass and shrinkage implemented). The long-dashed line corresponds to replacing the ordinary gluon distribution with the skewed one. The overall effect, an enhancement of approximately 10%, is seen strongest at high energies where the small dipoles

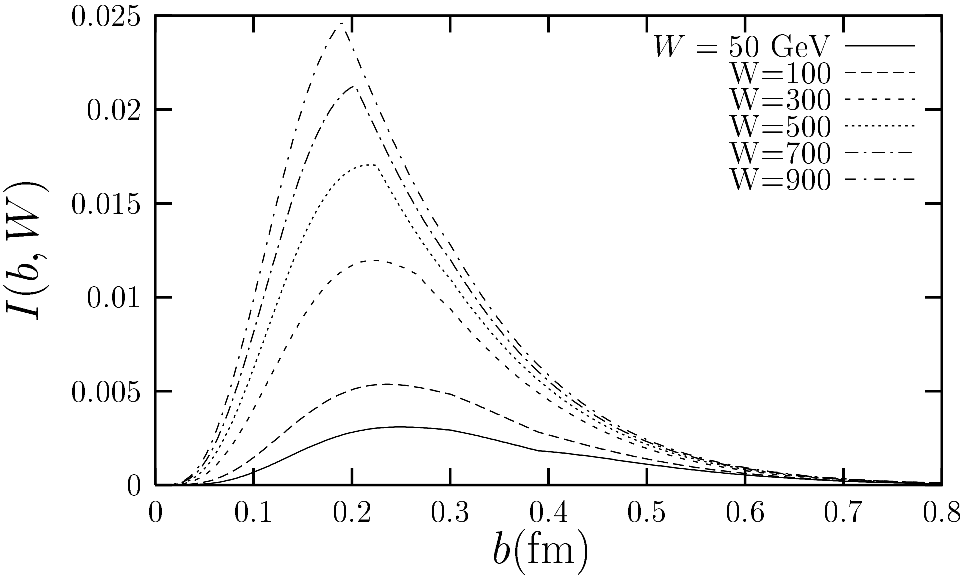

Figure 9: The evolution of the b-integrand with energy using skewed evolution and running quark mass in $\hat{\sigma}$. At high energies the effects of unitarity corrections are clearly seen in the shape.

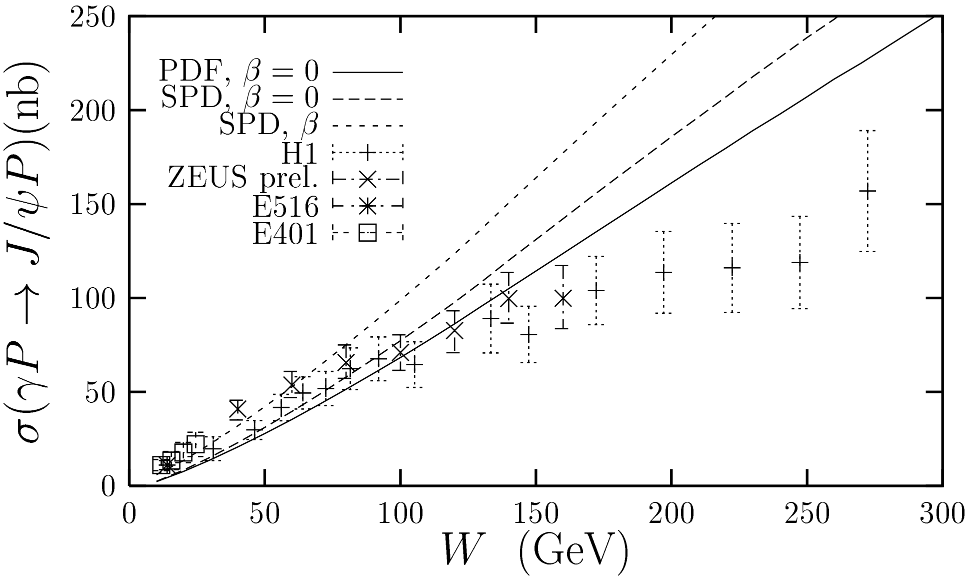

Figure 10: The effect of including both skewedness and β at the cross section level. The solid curve uses the ordinary gluon PDF with running mass and W-dependent slope included. The dashed curves include skewedness. The short-dashed curve also includes the real part of the amplitude.

play an increasingly important role (see figure 9). The shape in W still appears to be too steep. It is possible that if we allow unitarity corrections to play a role earlier we may be able to fit the high energy data better.

3.5 Including the real part of the amplitude

Having implemented the skewed gluon in the imaginary part of the amplitude we now reconstruct the real part using the analytic properties of the amplitude [33]. Numerically we achieve this by performing a two-power fit to $\mathcal{I}m\ A(W)$ over a very wide range in W ($10 < W < 900$ GeV) using the form

$$\mathcal{I}m\ A(W) = a_1 \left(\frac{W^2}{W_0^2}\right)^{p_1} + a_2 \left(\frac{W^2}{W_0^2}\right)^{p_2}, \tag{3.12}$$

the real part is then given by

$$\mathcal{R}e\ A(W) = a_1 \left(\frac{W^2}{W_0^2}\right)^{p_1} \tan\left(\frac{\pi p_1}{2}\right) + a_2 \left(\frac{W^2}{W_0^2}\right)^{p_2} \tan\left(\frac{\pi p_2}{2}\right). \tag{3.13}$$

The ratio of real to imaginary parts, β is then obviously given by

$$\beta = \frac{\tan(\pi p_1/2) + a_2/a_1\ (W^2/W_0^2)^{p_2-p_1} \tan(\pi p_2/2)}{1 + a_2/a_1\ (W^2/W_0^2)^{p_2-p_1}}. \tag{3.14}$$

This increases the normalization of the cross section by β^2% (cf. eq. (2.9)).

We achieve an excellent two-power fit using MINUIT [34] and get the following values for the fit parameters:

$$\begin{aligned} a_1 &= 0.00104\,, \qquad & a_2 &= -0.000794\,, \\ p_1 &= 0.226\,, \qquad & p_2 &= -0.0775\,. \end{aligned} \tag{3.15}$$

Figure 11 illustrates that β decreases as a function of W as the smaller power becomes less significant (see curves labelled $\lambda = 10$). The short dashed line of figure 10 shows the overall energy-dependent enhancement (about 20% at high energies) when this implemented at the cross section level. This improves the description of the low energy data and in terms of shape, but leads to a worse overshoot at high energies.

4. Decreasing λ and predictions for THERA

At large Q^2, within the leading and next-to-leading logarithmic approximations of perturbative QCD, there exists a rather straightforward relationship between transverse size and the relevant four-momentum scale for the process concerned, i.e. that they are inversely proportional [4, 5]. The constant of proportionality, λ, was determined in [4] by an iterative averaging procedure involving the integral in b for the structure function F_L: $\lambda = \langle b_{F_L} \rangle^2 Q^2$. A value of $\lambda \approx 9$ was obtained from this

JHEP03(2001)045

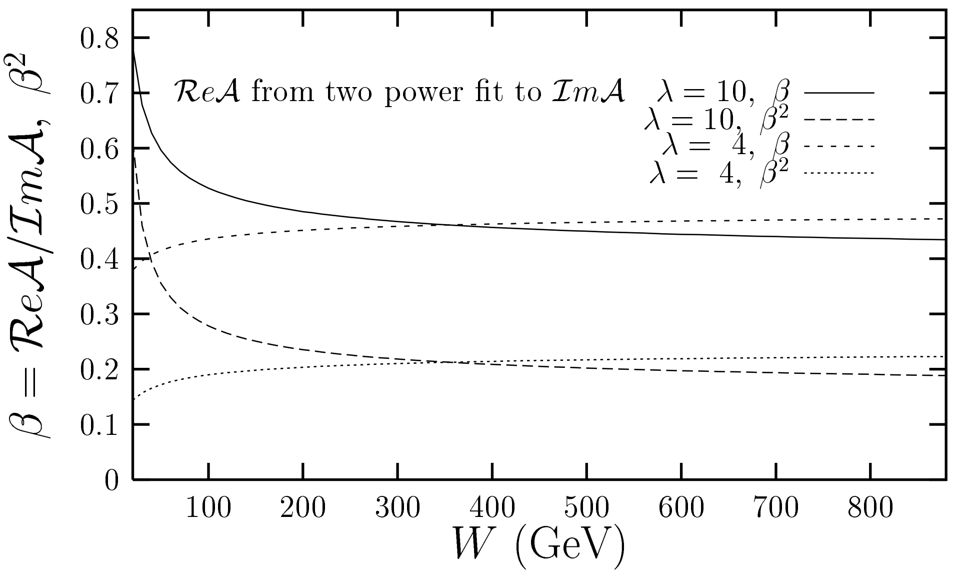

Figure 11: A plot to illustrate the relative size of the real part of the amplitude as a function of energy (for CTEQ4L partons). In the case $\lambda = 4$ a two-power fit to MINUIT fit produces two positive terms with positive powers, hence β calculated from the fit increases slightly as a function of energy (the fit parameters in this case are: $a_1 = 0.000386$, $p_1 = 0.291$, $a_2 = 0.000186$, $p_2 = 0.0272$).

method and this was found not to vary too much with x and Q^2 at small $x \approx 10^{-3}$, provided $Q^2 \gtrsim 10$ GeV^2. At larger b^2, where applicability of perturbative QCD can not be justified, this relationship may break down, i.e. λ may be found to depend on b^2 or equivalently on Q^2. Indeed, in [6] we observed that the value coming from this procedure was seen to deviate when a wider kinematic range was considered. During the work carried out for [12] it was found that although λ was changing, if kept within reasonable limits ($4 \lesssim \lambda \lesssim 15$) the result for F_L only changed by a few percent (see [12, figure 5] for an explanation of this approximate scaling). Having made this observation, a value of $\lambda = 10$ was chosen for convenience (and because it most closely corresponded with average value of b in F_L) in the analysis of inclusive Structure Functions.

At smaller Q^2, we need to account for non-perturbative QCD effects, where the relationship between b^2 and Q^2 is not so straightforward (in particular, b^2 does not tend to infinity as $Q^2 \to 0$). To account for this slower dependence on Q^2, for smaller Q^2, and to test the sensitivity to non-perturbative QCD effects we diminish λ at all b. It is logical that decreasing λ will have a much bigger effect on processes such as J/ψ photoproduction which contain greater contamination from large distances and are sensitive to scales at which the gluon density is changing rapidly at small x ($Q_0^2 < \bar{Q}^2 < 10\,\text{GeV}^2$).

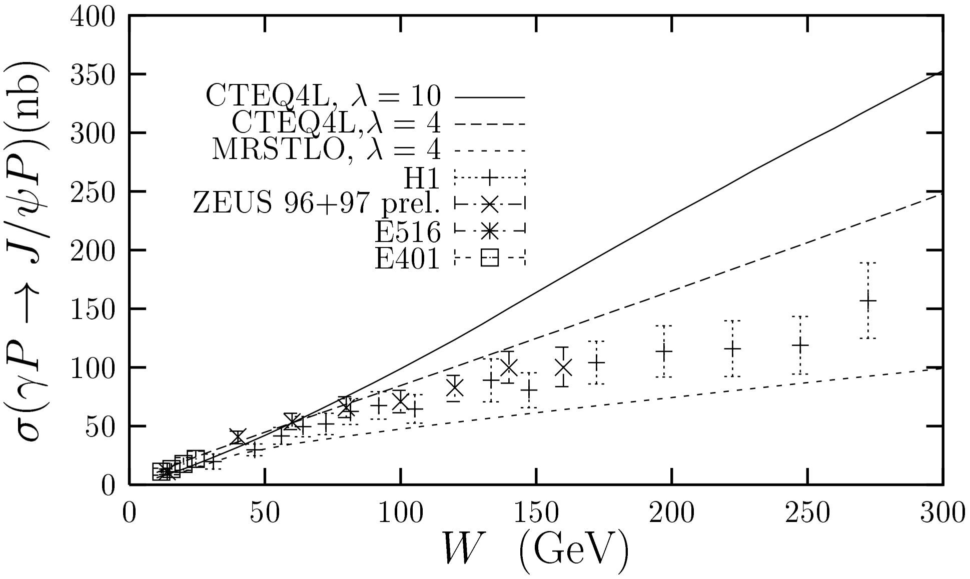

Figure 12: Decreasing the value of λ from 10 to 4 improves the agreement with data dramatically for CTEQ4L partons. The short-dashed implements MRST input partons, with $\lambda = 4$.

Changing the value of λ has several effects. Firstly, the position of the input scale, b_{Q0}, in b shifts which affects $\hat{\sigma}$ directly (recall that b_π which also specifies $\hat{\sigma}$ is fixed). It also directly influences the scales at which the gluon distribution is sampled, $\bar{Q}^2$ and x', (cf. eqs. (3.2), (3.9) and figures 4, 5). Since the light-cone wavefunctions do not depend on λ (except implicitly though the $\bar{Q}^2$-dependence of $m_{c,r}$), this change has the effect of squeezing or dilating the perturbative region in b. Decreasing λ decreases $b_{Q0} = \sqrt{\lambda}/Q_0$ and so diminishes the perturbative region almost without modifying $\hat{\sigma}$ in the perturbative regime. The effect on $\hat{\sigma}$ is explicitly illustrated in figure 13 which shows the dipole cross section for several values of x and $\lambda = 4, 10$ (for the purposes of this figure we neglect the 10% skewedness effect). This should make the cross section rise less steeply with energy as it enhances the non-perturbative piece. To test this we reran our code using the lowest value which left the results for F_L unaffected, i.e. $\lambda = 4$.[5]

The effect on the cross section was rather dramatic and is shown in figure 12 (the real part of the amplitude, calculated as described above, is included, cf. figure 11). The cross section is increased in the fixed target region and suppressed in the high energy region. Both effects move it in the direction of the data. From figure 13 we

[5]Incidentally and accidentally, this is the value advocated in the papers of Gotsman, Levin and Maor and collaborators for all Q^2. See [35] for the latest version of their model which includes shadowing corrections. It is applied to J/ψ production in [36].

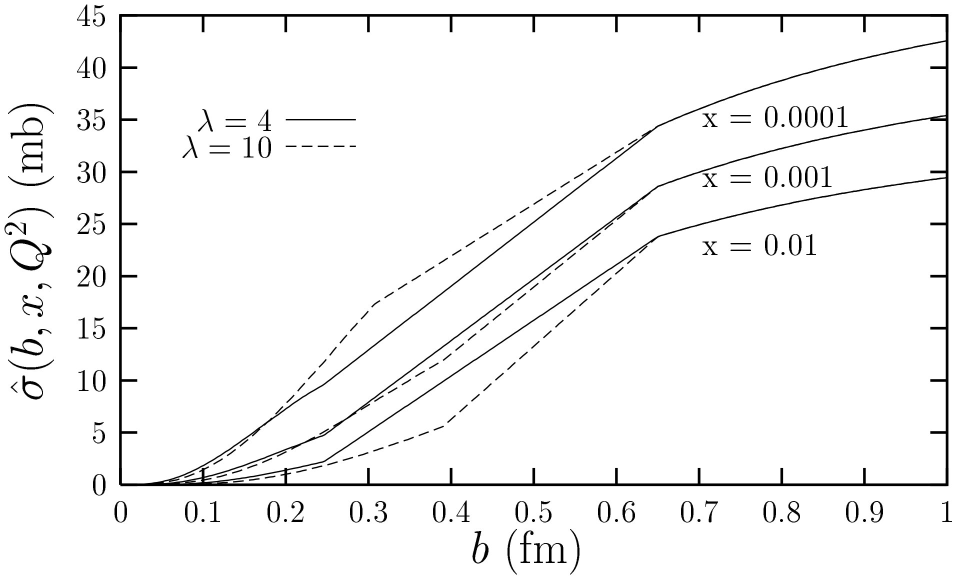

Figure 13: The interaction cross-section, $\hat{\sigma}$ for CTEQ4L, linear ansatz, for $x = 0.01, 0.001, 0.0001$, $\lambda = 4, 10$. A value of $Q^2 = Q_0^2 = 2.56\,\mathrm{GeV}^2$ is used in the ansatz for b-dependent scales in $\hat{\sigma}$.

can see that big differences between $\lambda = 4$ and $\lambda = 10$ only emerge in the region around $b = 0.3$ fm. Hence, for $200 < W < 300\,\mathrm{GeV}$, where the main contribution to the cross section originates from this region in b, the largest relative difference between the final cross sections is observed (see figure 12). The difference does not increase further with energy since the contribution from smaller b gradually becomes dominant (see figure 9).

As an additional cross check we re-examined our description of $F_2(x, Q^2)$, using $\lambda = 4$. The results for selected values of Q^2 are shown by the dashed lines in figure 14. A comparison with the solid lines ($\lambda = 10$) illustrates that F_2 is also fairly insensitive to this change in λ and we still provide a reasonable description of the HERA data. Also shown (dotted curves) is the evaluation of F_2 using the latest MRST leading-order gluon distribution [17], with $\lambda = 4$. This appears to get closer to the data than the earlier CTEQ4L distributions (at least in the deep inelastic region). Taken together both the MRST and CTEQ4L curves illustrate the spread of predictions available from modern leading-log fits and hence give some indication of the theoretical uncertainty of the description.

Extrapolating to higher energies we observe a rather broad spread of predictions for J/ψ-photoproduction in the THERA range in figure 15. Since, for CTEQ4L partons, the case $\lambda = 4$ does a better job on the lower energy data, we favour the dashed curve as our prediction for THERA. Despite the effect of the unitarity cor-

JHEP03(2001)045

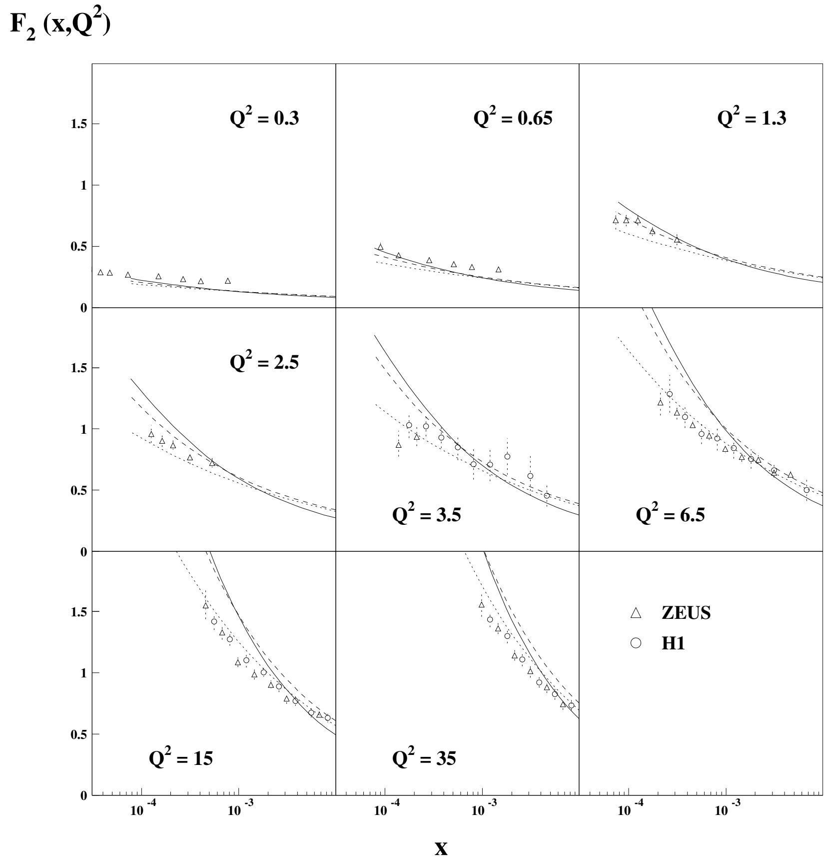

Figure 14: A comparison of the inclusive cross section F_2 using the dipole cross section with $\lambda = 4$ (dashed line) and $\lambda = 10$ (solid line), with a selection of the ZEUS [37] and H1 [38] data. Also shown (dotted curves) are the values obtained using leading-order MRST partons with $\lambda = 4$.

rection in the integrands, evident in figure 9, the overall taming effect on the energy dependence at the cross section level appears to be rather mild within the considered model. This is because the contribution of very small b for which taming is still not important becomes more and more significant as the energy increases. In order to illustrate the sensitivity of the predictions to the choice of input parton density set we also show in figures 12, 15 (short-dashed) curves for the latest MRST leading-order partons [16]. The latter assume an analytic form for the small-x behaviour of the input gluon which decreases as a function of $1/x$, which explains the milder energy dependence.

Small λ (e.g. 4-5) appear from the J/Ψ analysis to be required where large b is significant. This is strongly related to the relative influence of perturbative and non-perturbative contributions. It seems that the current uncertainty associated with the small-x gluon distribution prevent any strong statement being made about λ at small b. One may choose λ in the range 5-15 and the results for physical quantities don't change in quality (at present this applies to F_2 and hard vector meson production, since F_L is not yet measured). Making this change is perfectly allowed within the

JHEP03(2001)045

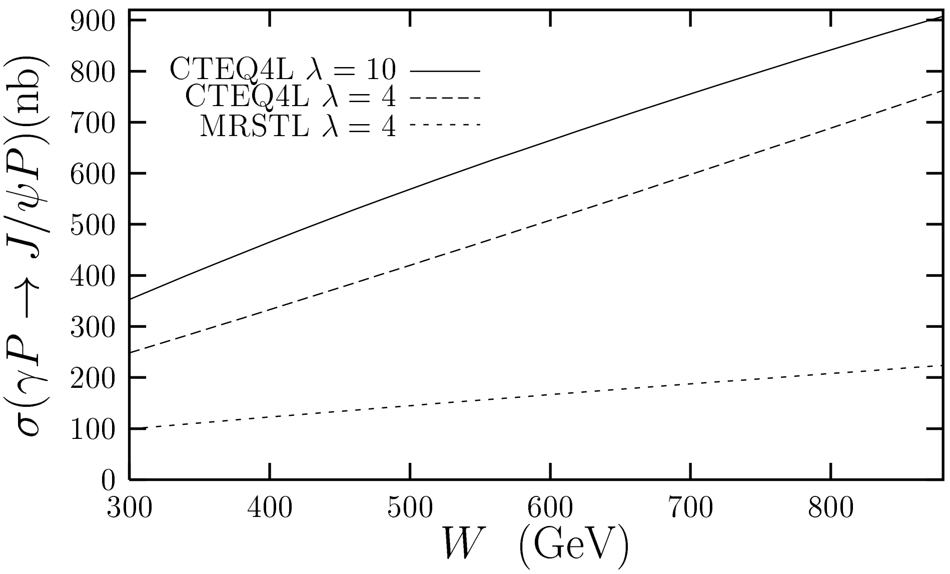

Figure 15: The photoproduction cross section for J/ψ in the THERA region using two different values for the scaling parameter λ and CTEQ4L partons. The short-dashed curve shows the prediction using MRST leading order partons and $\lambda = 4$.

leading-log accuracy of the model (it corresponds to an attempt to mimic some NLO corrections). This observation shows that an estimate of the region where unitarity corrections become significant [5, 12, 39] will contain large uncertainties before a NLO calculation of cross section is made.

5. Evaluation of $\alpha'_{I\!P}$

Since $\alpha'_{I\!P}$ is rather sensitive to the physics relevant for the taming of parton distributions, in this section we develop a more sophisticated approach to calculating it.

We would like to point out that the measurement of $\alpha'_{I\!P}$ recently reported by ZEUS [25] is entirely consistent with the results of our model. For large transverse sizes one expects a contribution of $\alpha'_{I\!P}(\text{soft}) = 0.25\,\text{GeV}^{-2}$, whereas for very small sizes a negligible contribution is expected. We can see this by introducing a simple, but reasonable, model based on dimension analysis:

$$\alpha'_{I\!P}(b) = 0.5\,\left(\frac{b^2}{b^2 + b_\pi^2}\right)\text{GeV}^{-2}\,. \tag{5.1}$$

This model is designed to give $\alpha'_{I\!P}(b = b_\pi) = \alpha'_{I\!P}(\text{soft}) = 0.25\,\text{GeV}^{-2}$, and to tend to zero quadratically at small b. There is a gradual decrease of $\alpha'_{I\!P}$ with increase of energy, as small b configurations become more important. We quantify this in

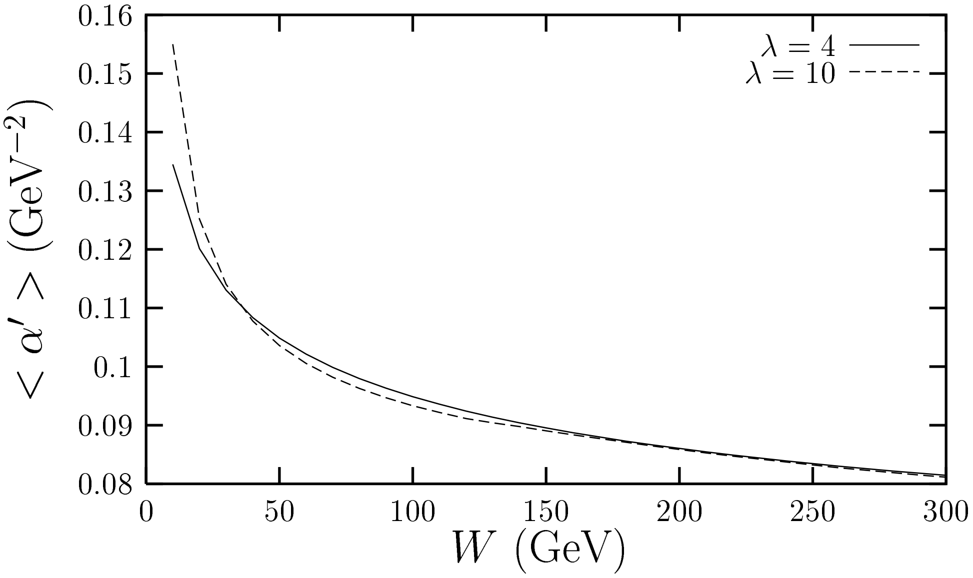

Figure 16: The average shrinkage parameter, α' (using the simple model of eq. (5.1)) as a function of W (GeV), for two values of λ.

figure 16 by plotting the energy dependence of the average of $\alpha'_{I\!P}$ defined as (cf. eq. (2.7))

$$\langle \alpha'_{I\!P} \rangle = \frac{\int b\ db\ \alpha'_{I\!P}(b) I_z(b) \hat{\sigma}}{\int b\ db\ I_z(b) \hat{\sigma}}\,, \tag{5.2}$$

for $\lambda = 4, 10$. We see that this model is in broad agreement with the ZEUS value [25, 26]: $\alpha'_{I\!P} = 0.098 \pm 0.035 \pm 0.05\,\mathrm{GeV}^{-2}$.

Strictly speaking, the energy dependence apparent in figure 16 may be slightly too strong when considering its effect on the t-slope parameter B. The average b, at a particular energy, is built in to the value of $B(W_0)$ at the normalization point (cf. eq. (3.6)), but is expected to decrease with energy. We illustrate the point using the following phenomenological parameterisation for the slope of t-dependence:

$$B(W^2, Q^2) = \frac{(\langle b^2 \rangle / 4 + r_N^2)}{3} + 2\alpha'_{I\!P} \ln W^2/W_0^2\,. \tag{5.3}$$

Here $\langle b^2 \rangle$ is the average distance between c and $\bar{c}$, defined in an analogous way to the average $\alpha'_{I\!P}$ (cf. eq. (5.2)). In this phenomenological model a possible presence of $\ln b^2/b_0^2$ terms is ignored. This formulae may be thought of as defining a convention for a new parameter, α', related directly to the logarithmic energy dependence of the slope parameter, B:

$$\alpha' \equiv \frac{\partial B}{\partial\ (4\ \ln(W/W_0))}\,,$$

$$\alpha' = \frac{\langle b^2(W)\rangle - \langle b^2(W_0)\rangle}{48 \ln W/W_0} + \alpha'_{I\!P}\,. \tag{5.4}$$

However, it turns out that in HERA kinematics the difference between α' and $\alpha'_{I\!P}$ from this effect is only about $-0.01\,\mathrm{GeV}^{-2}$.

Thus, the observed energy dependence of the average value of b in hard amplitudes (which are influenced by DGLAP evolution) leads to a more complicated and process-dependent energy dependence of the slope parameter, B, than that which is predicted by universal soft Pomeron exchange. At THERA energies and beyond, where the taming region starts to dominate, one expects that $\alpha'_{I\!P}$ should start to increase again.

In our picture we expect both B and $\alpha'_{I\!P}$ to change with energy and photon virtuality as the balance between short and long distance contributions shifts. A dedicated forward detector for measuring scattered protons, such as the one recently proposed by the H1 collaboration [40], would allow this issue to be investigated in detail.

6. Discussion and open questions

Using $\lambda = 4$ and CTEQ4L partons our model still seems to overshoot the available data somewhat (cf. long-dashed line in figure 12), whereas MRST undershoot ((cf. short-dashed line). We would like to reiterate the point that the gluon distribution at small $x \approx 10^{-4}$ is not very well constrained by the current data (which mainly provides an indirect constraint via DGLAP-driven scaling violations of F_2). This fact is reflected in the wide spread of numerical values for the gluon distribution at small x in the currently available partons distributions,[6] of which we have shown only two here. Hence we are not too concerned by the fact that our curve appears to overshoot particularly the H1 data [24] at the highest HERA energies using CTEQ4L. The framework we have described is general and can clearly use any leading-log parton density set that is available. However, we are encouraged by the improvement in agreement in the overall shape, which allows us to get closer to the data over a wide range in energy.

It is natural to ask if higher order Fock states ($|c\bar{c}g\rangle$ etc), which are only formally suppressed by α_s, are important in the photoproduction of J/ψ. The rationale employed in [4] was that using the solution to the Schrödinger equation (boosted to light cone) should take into account the most important corrections for large transverse distances. Recent studies of the effect of radiative corrections on the leptonic decay width [22] indicate that perturbative corrections for small distances may well be large. At present it is unclear what effect this will have on the photoproduction of J/ψ. From the theoretical side what is required is a complete next-to-leading-log calculation. This question could be addressed phenomenologically by examining

[6] See http://durpdg.dur.ac.uk/HEPDATA/PDF3.html

the relative characteristics of various diffractive charm measurements (exclusive J/ψ, J/ψ + 1 jet, and open charm). The question is even more urgent in the case of ψ' which is obviously a larger bound state and contains a node.

7. Conclusions

We have investigated the photoproduction of J/ψ in the context of the QCD-improved dipole model introduced in [12]. This model directly incorporates a contribution from long distances which is responsible for the low energy production. As the energy increases, the short distance mechanism of perturbative two-gluon exchange becomes increasingly important. Overall our description of the data over the whole measured range is improved relative to analyses which only take the perturbative contribution into account. At very high energies we incorporate taming or unitarity corrections and present predictions for the cross section in the THERA range ($250 < W < 900$ GeV). In our model, unitarity corrections affect smaller and smaller transverse sizes at progressively higher energies. For J/ψ photoproduction, which is sensitive to a broad range in transverse sizes, it turns out that in the THERA region there is always a significant contribution to the cross section that rise quickly with energy. This implies that the taming of the growth of the cross section with energy is rather gradual (the precise details depend on the choice of input density).

We show that the skewedness of the amplitude induces a relatively small enhancement in the cross section (approximately 10%). This effect is likely to be swamped by other uncertainties associated with the t-dependence and the light-cone wavefunction of the vector meson.

Of much greater numerical importance in describing the available data is to modify the balance between short and long distances contributions. In our model, this may be controlled by changing the scaling parameter λ which sets the relationship between four-momentum scales and transverse sizes in the interaction cross section. For CTEQ4L partons, the shape in energy of the J/ψ photoproduction data appears to favour a change to a lower value ($\lambda = 4$) for large b than that which was derived in [4, 5, 12] for small b ($\lambda = 10$). The quality of the description of the structure function F_2 is relatively unchanged by this modification. The largest uncertainty comes from poor knowledge of the numerical size of the leading-log small-x gluon distribution. This leads to a rather broad band of predictions for J/ψ photoproduction in THERA region. Studies of the photo- and electroproduction of other vector mesons, within the same framework, is underway.

Acknowledgments

We thank Sandy Donnachie, Vadim Guzey and Andreas Freund for useful contributions. We would also like to thank the referee for his helpful comments which led to several improvements to this text.

References

[1] L. Frankfurt and M. Strikman, *Large t, triple pomeron diffractive processes in QCD*, *Phys. Rev. Lett.* **63** (1989) 1914.

[2] M.G. Ryskin, *Diffractive J/ψ electroproduction in lla QCD*, *Z. Physik* **C 57** (1993) 89;
A.D. Martin, M.G. Ryskin and T. Teubner, *The QCD description of diffractive ρ meson electroproduction*, *Phys. Rev.* **D 55** (1997) 4329 [hep-ph/9609448]; *Diffractive electroproduction of ρ meson excitations*, *Phys. Rev.* **D 56** (1997) 3007 [hep-ph/9701366]; *Υ photoproduction at HERA compared to estimates of perturbative QCD*, *Phys. Lett.* **B 454** (1999) 339 [hep-ph/9901420].

[3] S.J. Brodsky, L. Frankfurt, J.F. Gunion, A.H. Mueller and M. Strikman, *Diffractive leptoproduction of vector mesons in QCD*, *Phys. Rev.* **D 50** (1994) 3134 [hep-ph/9402283].

[4] L. Frankfurt, W. Koepf and M. Strikman, *Hard diffractive electroproduction of vector mesons in QCD*, *Phys. Rev.* **D 54** (1996) 3194 [hep-ph/9509311].

[5] L. Frankfurt, W. Koepf and M. Strikman, *Diffractive heavy quarkonium photo- and electroproduction in QCD*, *Phys. Rev.* **D 57** (1998) 512 [hep-ph/9702216].

[6] L.L. Frankfurt, M.F. McDermott and M. Strikman, *Diffractive photoproduction of upsilon at HERA*, *J. High Energy Phys.* **02** (1999) 002 [hep-ph/9812316].

[7] K. Suzuki, A. Hayashigaki, K. Itakura, J. Alam and T. Hatsuda, *Validity of the color dipole approximation for diffractive production of heavy quarkonium*, *Phys. Rev.* **D 62** (2000) 031501 [hep-ph/0005250].

[8] P. Hoyer and S. Peigne, *$\psi' \to \psi$ ratio in diffractive photoproduction*, hep-ph/9909519.

[9] J.C. Collins, L. Frankfurt and M. Strikman, *Factorization for hard exclusive electroproduction of mesons in QCD*, *Phys. Rev.* **D 56** (1997) 2982 [hep-ph/9611433].

[10] J.C. Collins and A. Freund, *Proof of factorization for deeply virtual compton scattering in QCD*, *Phys. Rev.* **D 59** (1999) 074009 [hep-ph/9801262].

[11] A. Donnachie and P.V. Landshoff, *Exclusive vector photoproduction: confirmation of Regge theory*, *Phys. Lett.* **B 478** (2000) 146 [hep-ph/9912312]; *Small x: two pomerons!*, *Phys. Lett.* **B 437** (1998) 408 [hep-ph/9806344].

[12] M. McDermott, L. Frankfurt, V. Guzey and M. Strikman, *Unitarity and the QCD-improved dipole picture*, *Eur. Phys. J.* **C 16** (2000) 641 [hep-ph/9912547].

[13] B. Blattel, G. Baym, L. Frankfurt and M. Strikman, *Correlations and fluctuations in high-energy nuclear collisions*, *Phys. Rev.* **C 52** (1995) 1604 [nucl-th/9502038];
L. Frankfurt, A. Radyushkin and M. Strikman, *Interaction of small size wave packet with hadron target*, *Phys. Rev.* **D 55** (1997) 98 [hep-ph/9610274].

[14] H.L. Lai et al., *Improved parton distributions from global analysis of recent deep inelastic scattering and inclusive jet data*, *Phys. Rev.* **D 55** (1997) 1280 [hep-ph/9606399].

[15] V.N. Gribov and L.N. Lipatov, *Deep inelastic ep scattering in perturbation theory*, *Sov. J. Nucl. Phys.* **15** (1972) 438; *e^+e^- pair annihilation and deep inelastic ep scattering in perturbation theory*, *Sov. J. Nucl. Phys.* **15** (1972) 675;
Yu. L. Dokshitzer, *Calculation of the structure functions for deep inelastic scattering and e^+e^- annihilation by perturbation theory in quantum chromodynamics*, *Sov. Phys. JETP* **46** (1977) 641;
G. Altarelli and G. Parisi, *Asymptotic freedom in parton language*, *Nucl. Phys.* **B 126** (1977) 298.

[16] R.G. Roberts, private communication.

[17] A.D. Martin, R.G. Roberts, W.J. Stirling and R.S. Thorne, *Scheme dependence, leading order and higher twist studies of MRST partons*, *Phys. Lett.* **B 443** (1998) 301 [hep-ph/9808371].

[18] K. Golec-Biernat and M. Wüsthoff, *Saturation effects in deep inelastic scattering at low Q^2 and its implications on diffraction*, *Phys. Rev.* **D 59** (1999) 014017 [hep-ph/9807513];
K. Golec-Biernat and M. Wüsthoff, *Saturation in diffractive deep inelastic scattering*, *Phys. Rev.* **D 60** (1999) 114023 [hep-ph/9903358];
J.R. Forshaw, G. Kerley and G. Shaw, *Extracting the dipole cross-section from photo- and electro-production total cross-section data*, *Phys. Rev.* **D 60** (1999) 074012 [hep-ph/9903341];
J. Forshaw, G. Kerley and G. Shaw, *Predicting $F_2^{D(3)}$ from the dipole cross-section*, *Nucl. Phys.* **A 675** (2000) 80C [hep-ph/9910251];
E. Gotsman, E. Levin, U. Maor and E. Naftali, *The effect of screening on the x and Q^2 behaviour of F_2 slopes*, *Nucl. Phys.* **B 539** (1999) 535 [hep-ph/9808257];
E. Gotsman, E. Levin, U. Maor and E. Naftali, *Total $\gamma^* p$ cross section*, *Eur. Phys. J.* **C 10** (1999) 689 [hep-ph/9904277] and references therein.

[19] M.F. McDermott, *The dipole picture of small-x physics (a summary of the Amirim meeting)*, hep-ph/0008260.

[20] H. Cheng and T.T. Wu, *Expanding protons: scattering at high-energies*, MIT-Press, Cambridge, USA 1987.

[21] W. Buchmüller and S.H.H. Tye, *Quarkonia and quantum chromodynamics*, *Phys. Rev.* **D 24** (1981) 132.

[22] F.J. Yndurain, *Heavy quarkonium*, hep-ph/9910399;
Nucl. Phys. **93** *(Proc. Suppl.)* (2001) 196.

[23] E516 collaboration, *Inelastic and elastic photoproduction of J/ψ (3097)*, *Phys. Rev. Lett.* **52** (1984) 795;

E401 collaboration, *J/ψ photoproduction from 60 GeV/c to 300 GeV/c*, *Phys. Rev. Lett.* **48** (1982) 73.

[24] H1 collaboration, *Elastic photoproduction of J/ψ and Υ mesons at HERA*, *Phys. Lett.* **B 483** (2000) 23 [hep-ex/0003020].

[25] A. Bruni, on behalf of ZEUS and H1 collaborations, *Elastic J/ψ, ψ (2s) and Υ photoproduction at HERA*, Proc. DIS 2000, Liverpool April 2000, J.A. Gracey and T. Greenshaw eds., World Scientific, 2001.

[26] ZEUS collaboration, *Exclusive photoproduction of J/ψ mesons*, Abstract 878, submitted paper to XXXth ICHEP, Osaka, Japan July 2000.

[27] M. Klein, *THERA - electron-proton scattering at $\sqrt{s} \simeq 1$ TeV*, Proc. DIS 2000, Liverpool April 2000, J.A. Gracey and T. Greenshaw eds., World Scientific, 2001; see also http://www.ifh.de/thera/.

[28] M.E. Peskin and D.V. Schroeder, *An introduction to quantum field theory*, Addison-Wesley, Reading, USA 1995.

[29] X.-D. Ji, *Off forward parton distributions*, *J. Phys.* **G 24** (1998) 1181 [hep-ph/9807358].

[30] A. V. Efremov and A. V. Radyushkin, *Asymptotical behavior of pion electromagnetic form-factor in QCD*, *Theor. Math. Phys.* **42** (1980) 97; *Factorization and asymptotical behavior of pion form-factor in QCD*, *Phys. Lett.* **B 94** (1980) 245;
G.P. Lepage and S.J. Brodsky, *Exclusive processes in quantum chromodynamics: evolution equations for hadronic wave functions and the form-factors of mesons*, *Phys. Lett.* **B 87** (1979) 359; *Exclusive processes in perturbative quantum chromodynamics*, *Phys. Rev.* **D 22** (1980) 2157.

[31] A. Freund and V. Guzey, *Study of nondiagonal parton distribution models*, *Phys. Lett.* **B 462** (1999) 178 [hep-ph/9806267]; *Numerical methods in the lo evolution of nondiagonal parton distributions: the DGLAP case*, hep-ph/9801388.

[32] CTEQ collab., see http://www.phys.psu.edu/~cteq/#PDFs.

[33] V.N. Gribov and A.A. Migdal, *Properties of the pomeranchuk pole and the branch cuts related to it at low momentum transfer*, *Sov. J. Nucl. Phys.* **8** (1969) 583.

[34] F. James, *MINUIT: functional minimization and error analysis*, CERN Program Library Long Writeup, **D506**.

[35] E. Gotsman, E. Levin, M. Lublinsky, U. Maor and K. Tuchin, *Energy dependence of $\sigma^{\rm DD}/\sigma_{\rm tot}$ in DIS and shadowing corrections*, hep-ph/0007261.

[36] E. Gotsman, E. Ferreira, E. Levin, U. Maor and E. Naftali, *Screening corrections in DIS at low Q^2 and x*, hep-ph/0007274.

[37] ZEUS collaboration, *Measurement of the F_2 structure function in deep inelastic e^+p scattering using 1994 data from the Zeus detector at HERA*, *Z. Physik* **C 72** (1996) 399 [hep-ex/9607002]; *Measurement of the proton structure function F_2 at very low Q^2 at HERA*, *Phys. Lett.* **B 487** (2000) 53 [hep-ex/0005018].

[38] H1 collaboration, *A measurement and QCD analysis of the proton structure function $F_2(x, Q^2)$ at HERA*, *Nucl. Phys.* **B 470** (1996) 3 [hep-ex/9603004].

[39] H. Abramowicz, L. Frankfurt and M. Strikman, *Interplay of hard and soft physics in the small x deep inelastic processes*, DESY-95-047, Mar, 1995, 60pp., Published in *Surveys High Energ. Phys.* **11** (1997) 51, and *SLAC Summer Inst. 1994* **QCD161:S76** (1994) 539.

[40] H1 collaboration, L. Favart, *Proposal for a very forward proton spectrometer in H1 after 2000*, Proc. DIS 2000, Liverpool April 2000, J.A. Gracey and T. Greenshaw eds., World Scientific, 2001, p. 618 [hep-ph/0006167]; see also http://web.iihe.ac.be/h1pots.

JHEP03(2001)045